

Ligand Design | Hot Paper |

Cooperative H₂ Activation on Dicopper(I) Facilitated by Reversible Dearomatization of an “Expanded PNP Pincer” LigandErrikos Kounalis,^[a] Martin Lutz,^[b] and Daniël L. J. Broere*^[a]

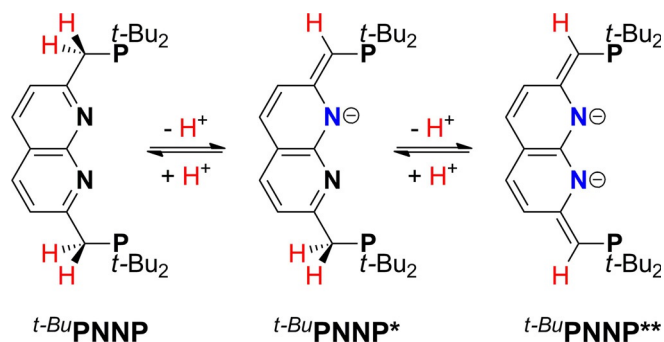
Abstract: A naphthyridine-derived expanded pincer ligand is described that can host two copper(I) centers. The proton-responsive ligand can undergo reversible partial and full dearomatization of the naphthyridine core, which enables cooperative activation of H₂ giving an unusual butterfly-shaped Cu₄H₂ complex.

Nature has evolved a variety of metalloenzymes that catalyze challenging chemical transformations by using earth-abundant metals under mild conditions. In several enzymes, the active site features complex architectures that enable multiple metals and ligands to work together to facilitate bond activation processes that are essential to enzyme function.^[1] Drawing inspiration from nature, various research groups have developed synthetic systems in which metals and ligands cooperatively activate chemical bonds.^[2] A prominent platform that enables such metal–ligand cooperativity (MLC) is the lutidine-derived PNP pincer^[3] ligand, and derivatives thereof, which enable cooperative substrate activation through reversible dearomatization of the heteroaromatic core. This MLC has been thoroughly studied and employed in catalysis by the Milstein group and others.^[4]

Another avenue in cooperative bond activation involves complexes in which multiple metal centers are in close proximity and work together to make or break chemical bonds.^[5] Ligands derived from 1,8-naphthyridine have been shown to be well-suited to place two metals in an orientation that enables metal–metal cooperativity (MMC).^[6] The Tilley group has reported aryl group transfer reactions^[7] and remarkable stabilization

of alkyl ligands^[8] on dinuclear copper complexes bearing a naphthyridine bis(dipyridyl) ligand.^[9] The Uyeda group has demonstrated that dinuclear metal complexes bearing redox-active naphthyridine diimine ligands can catalyze a variety of chemical transformations for which the MMC is essential for activity or selectivity.^[10] Very recently, the same group reported that these dinuclear systems can catalyze the reductive [4+1] cycloaddition of vinylidenes and dienes.^[11] Both the MMC and the redox-active nature of the ligand^[12] were found to be crucial for the observed reactivity. This demonstrates the potential for combining other types of cooperative elements in naphthyridine-derived ligands. However, to the best of our knowledge there are no examples where these dinucleating ligands display MLC beyond being redox active.^[13]

Our group is currently exploring ligand systems that can both host multiple low-valent first-row transition metals and also contain fragments that enable metal–ligand cooperativity. In this work, we describe the synthesis of a dinucleating naphthyridine diphosphine ligand (^t-BuPNNP, Scheme 1), which can



Scheme 1. The dinucleating “expanded pincer” ligand ^t-BuPNNP and the partial and full dearomatization upon single and double deprotonation, respectively.

bind two copper(I) centers in close proximity to each other. The so-called “expanded pincer” ligand in the corresponding dicopper(I) complexes can undergo reversible single and double deprotonation of the ligand concomitant with partial (^t-BuPNNP*) and full (^t-BuPNNP**) dearomatization of the naphthyridine core, respectively (Scheme 1). Moreover, we demonstrate how the expanded pincer ligand enables cooperative activation of H₂ on dicopper(I) and induces formation of a new type of copper hydride.

The expanded pincer ligand ^t-BuPNNP was prepared as an air-sensitive off-white solid through a three-step procedure

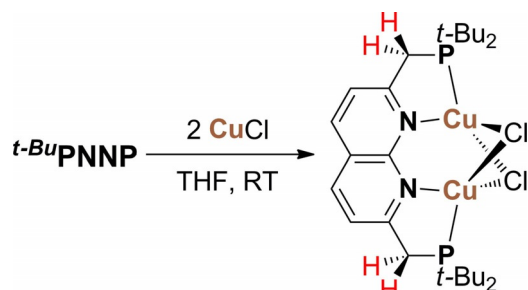
[a] E. Kounalis, Dr. Ing. D. L. J. Broere
Organic Chemistry and Catalysis, Debye Institute for Nanomaterials Science
Faculty of Science, Utrecht University
Universiteitsweg 99, 3584 CG, Utrecht (The Netherlands)
E-mail: d.l.j.broere@uu.nl

[b] Dr. M. Lutz
Crystal and Structural Chemistry, Bijvoet Center for Biomolecular Research
Faculty of Science, Utrecht University
Padualaan 8, 3584 CH Utrecht (The Netherlands)

Supporting information and the ORCID identification number(s) for the author(s) of this article can be found under:
<https://doi.org/10.1002/chem.201903724>.

© 2019 The Authors. Published by Wiley-VCH Verlag GmbH & Co. KGaA.
This is an open access article under the terms of Creative Commons Attribution NonCommercial License, which permits use, distribution and reproduction in any medium, provided the original work is properly cited and is not used for commercial purposes.

from commercially available reagents in 11% overall yield.^[14] The ¹H, ¹³C and ³¹P NMR spectra of ^t-BuPNNP in CD₂Cl₂ at 298 K show the expected number of resonances for a C_{2v} symmetric species. The ³¹P{¹H} NMR spectrum shows a single resonance at δ = 35.8 ppm, similar to the lutidine-derived ^t-BuPNP pincer ligand.^[15] Reacting ^t-BuPNNP with two equiv of CuCl in THF gives dinuclear complex **1** (Scheme 2), which was isolated as a

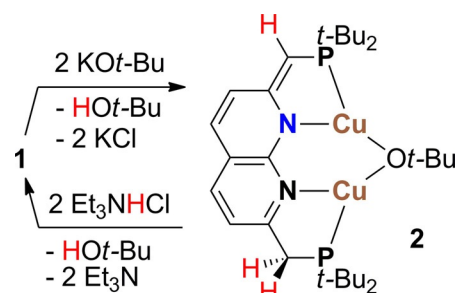


Scheme 2. Synthesis of dinuclear complex **1**.

pink solid in 78% yield. The ¹H, ¹³C and ³¹P NMR spectra of **1** in CD₂Cl₂ at 298 K show that the C_{2v} symmetry is retained upon binding two Cu centers. The ³¹P{¹H} NMR spectrum shows a single broad resonance at δ = 26.1 ppm, consistent with binding of the phosphines to Cu.^[16] The broadness of the resonance is common for Cu(I) phosphine complexes, due to quadrupolar relaxation arising from ⁶³Cu and ⁶⁵Cu (both I = 3/2) nuclei.^[17]

Layering a CH₂Cl₂ solution of **1** with hexane yielded crystals suitable for single-crystal X-ray diffraction. The solid-state structure (Figure 1, left) confirmed the presence of two Cu centers separated by 2.581(4) Å within the expanded pincer ligand. The Cu centers are equivalent by symmetry (Z' = 0.5) and show a distorted tetrahedral geometry.

Treatment of complex **1** with two equiv^[18] KO^t-Bu at room temperature gives complex **2** (Scheme 3), which was isolated as a vivid red solid in 90% yield. The ³¹P{¹H} NMR spectrum of **2** in C₆D₆ at 298 K features two broad resonances at δ = 26.9 and 7.7 ppm, showing two magnetically inequivalent phosphorus atoms. This loss of symmetry in **2** is also evident in the ¹H spectrum, which shows the expected increase in aromatic sig-



Scheme 3. Reversible deprotonation of **1** to give **2**.

nals for an unsymmetrically substituted naphthyridine, and an additional singlet at δ = 1.88 ppm, which we assign to the μ₂-Ot-Bu ligand. In addition, a two-proton doublet at δ = 2.57 ppm (J_{PH} = 7.4 Hz) and a one-proton doublet at δ = 4.29 ppm (J_{PH} = 1.8 Hz) agree with a partially dearomatized ^t-BuPNNP* ligand. These observations are comparable to those made upon dearomatization of related mononuclear complexes bearing lutidine-derived PNP pincer ligands.^[19]

Crystals suitable for single-crystal X-ray diffraction were obtained from a concentrated pentane solution of **2** at -40 °C. Two independent molecules of **2** were found in the asymmetric unit (Z' = 2). Each molecule features a ^t-BuPNNP* ligand bound to two copper centers that display distorted trigonal planar geometries and a μ₂-Ot-Bu ligand (Figure 1, middle). A notable feature are the Cu...Cu distances in the two molecules [3.0467(2) and 3.0218(2) Å], which are approximately 0.4 Å longer than that observed in **1**. This is likely a result of the bulky μ₂-Ot-Bu ligand, and it shows that the expanded pincer ligand allows for flexibility towards hosting two metals at varying distances. Partial dearomatization of the naphthyridine is evident by the double bond character of the C1–C2 bonds (see Table 1), which are shorter by approximately 0.14 Å than the C9–C10 bonds, and the C1–C2 bond in **1**. In addition, the observed metric parameters suggest localized double C3–C4 bonds and single C2–C3 and C4–C5 bonds, which contrasts with the delocalized C5–C7, C7–C8 and C8–C9 bonds (all ~1.38 Å). Interestingly, the partial dearomatization makes both PN binding pockets distinct within the ^t-BuPNNP* ligand. On the dearomatized sides, the Cu1–N1 distances are slightly

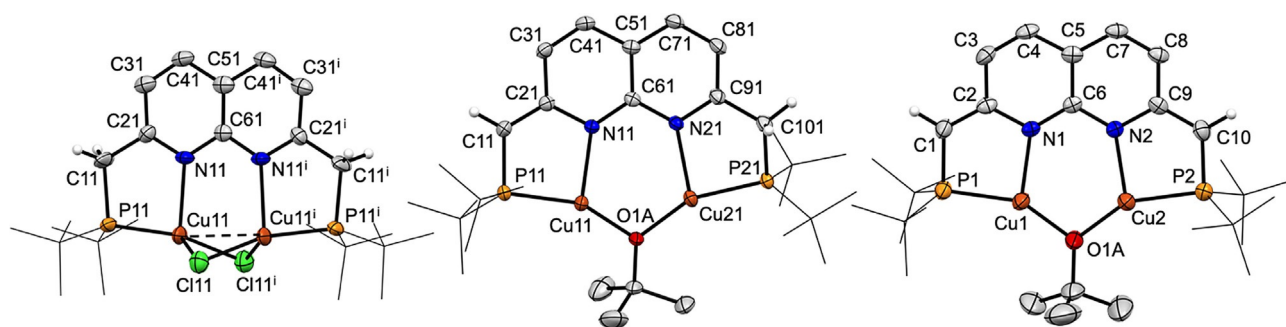


Figure 1. Displacement ellipsoid plots (50% probability) of complex **1** (left, symmetry code *i*: 1–*x*, –*y*, *z*), **2** (middle), and the anion of **3** (right). Most hydrogen atoms, and cations (for **3**) are omitted, and *t*-Bu groups on P are depicted as wireframe for clarity. For **2** only one molecule in the asymmetric unit is depicted. For **1** and **3**, only the major disorder component is shown.

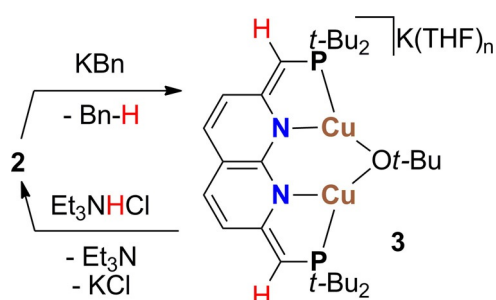
Table 1. Selected distances and angles of compounds **1–3** in Å and °, respectively.

Atoms	1	2 ^[a]	3	3–18 c6
Cu–Cu	2.581(4)	3.0467(2)	3.0218(2)	2.9259(6)
P1–Cu1	2.186(3)	2.1807(4)	2.1740(4)	2.1818(10)
P2–Cu2	2.186(3) ^[b]	2.1650(4)	2.1737(4)	2.1815(10)
N1–Cu1	2.204(7)	2.1277(11)	2.1259(11)	2.081(3)
N2–Cu2	2.204(7) ^[b]	2.1870(11)	2.1638(11)	2.104(3)
Cu1–O1	–	1.8929(10)	1.8915(10)	1.907(5) ^[c]
Cu2–O1	–	1.8761(10)	1.8880(9)	1.897(5) ^[c]
C1–P1	1.837(10)	1.7770(14)	1.7753(14)	1.754(4)
C10–P2	1.837(10) ^[b]	1.8338(15)	1.8444(14)	1.751(4)
C1–C2	1.515(12)	1.3743(19)	1.3782(19)	1.380(5)
C2–C3	1.403(9)	1.4542(19)	1.4539(18)	1.440(5)
C3–C4	1.362(10)	1.339(2)	1.340(2)	1.351(5)
C4–C5	1.442(9)	1.431(2)	1.435(2)	1.411(5)
C5–C6	1.366(12)	1.4345(18)	1.4345(18)	1.434(5)
C5–C7	1.442(9) ^[b]	1.3840(19)	1.386(2)	1.400(5)
C7–C8	1.362(10) ^[b]	1.382(2)	1.385(2)	1.352(5)
C8–C9	1.403(9) ^[b]	1.388(2)	1.387(2)	1.432(5)
C9–C10	1.515(12) ^[b]	1.515(2)	1.513(2)	1.399(5)
C2–N1	1.327(10)	1.3974(17)	1.3887(17)	1.391(4)
N1–C6	1.361(8)	1.3507(16)	1.3503(17)	1.391(4)
C6–N2	1.327(10) ^[b]	1.3731(17)	1.3701(17)	1.366(4)
N2–C9	1.361(8) ^[b]	1.3558(17)	1.3578(17)	1.386(4)
P1–C1–C2	115.6(6)	120.57(11)	119.35(10)	120.4(3)
P2–C10–C9	115.6(6) ^[b]	112.66(9)	112.10(9)	121.0(3)

[a] Two independent molecules in the asymmetric unit. [b] The molecule has exact C_2 symmetry. Only half of the parameters are independent. [c] Major disorder component.

shorter (Table 1) than observed for Cu2–N2, in agreement with the expected increase of negative charge on N1. Moreover, nearly flat five-membered metallacycles are observed wherein the Cu1 atoms are located within the naphthyridine planes. In the other PN pockets, the Cu2 and P2 atoms are found sticking out of the naphthyridine planes, likely facilitated by the more flexible methylene linker.

Treatment of complex **2** with 2 equiv of Et_3NHCl results in quantitative reformation of **1** and $\text{HO}t\text{-Bu}$, showing that the observed partial dearomatization is reversible. Reacting **2** with 1 equiv benzyl potassium (KBn) at room temperature gives **3** (Scheme 4), which was isolated as an orange film in 95% yield. The $^{31}\text{P}\{^1\text{H}\}$ NMR spectrum of **3** in $[\text{D}_8]\text{THF}$ at 298 K shows a single resonance at $\delta = 14.4$ ppm indicating two magnetically equivalent phosphorus atoms. This gain in symmetry for **3**



Scheme 4. Reversible deprotonation of **2** to give **3**.

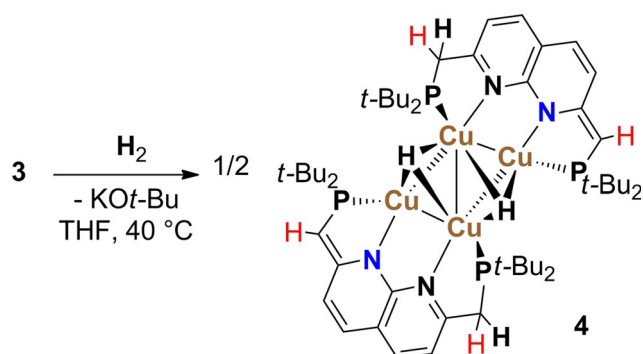
compared to **2** is also evident in the ^1H and ^{13}C NMR spectra, which show the expected number of resonances for a C_{2v} symmetric species. Notably, the resonances corresponding to the naphthyridine protons in the ^1H NMR spectrum are significantly shifted upfield to $\delta = 6.12$ and 5.56 ppm, and integrate equally to a doublet ($J_{\text{PH}} = 1.3$ Hz) at $\delta = 3.27$ ppm, which we assign to the deprotonated methylene linkers in the $t\text{-BuPNNP}^{**}$ ligand. Together, these observations support full dearomatization of the naphthyridine core of the ligand.

Crude **3** is soluble in various nonpolar solvents (e.g., pentane and Et_2O) and tends to precipitate, oil out or remain in solution. Fortunately, addition of 1 equiv of 18-crown-6 to a solution of **3** gives a species (**3–18 c6**) that displays nearly identical NMR spectra in $[\text{D}_8]\text{THF}$ solution, yet is far less soluble in nonpolar solvents. Crystals of **3–18 c6** suitable for single-crystal X-ray diffraction were obtained from a solution of **3** with 1 equiv 18-crown-6 in a THF/pentane mixture at -40°C .

The solid-state structure (Figure 1, right) revealed a flat fully dearomatized $t\text{-BuPNNP}^{**}$ ligand that holds the $\text{Cu}_2(\mu_2\text{-Ot-Bu})$ core in the naphthyridine plane. The anionic complex is separated from the potassium cation, which is sequestered by 18-crown-6 and two THF molecules. In agreement with the NMR spectra, the metric parameters reveal a fully dearomatized ligand where both halves of the $t\text{-BuPNNP}^{**}$ ligand have localized double bonds between C1–C2, C3–C4, C7–C8 and C9–C10 (see Table 1). Deprotonation of both arms of related lutidine-based pincer ligands is possible, but typically results in complexes that are too sensitive for isolation.^[20]

With the series of complexes **1–3** in hand, some clear trends in metric parameters (Table 1 and Figure S28) can be observed that reflect the extent of dearomatization. The increased ionic character on N1 and N2 upon partial and full dearomatization results in shortening of N–Cu distances, as expected. However, between **1–3** the P–Cu distances do not differ significantly, which is also the case for the Cu– μ_2 -O distances between **2** and **3**. The most notable changes upon dearomatization are the shorter C1–C2/C9–C10 (~ 0.14 Å) and C1–P1/C10–P2 (~ 0.07 Å) distances. Additionally, the P1–C1–C2 and P2–C10–C9 angles increase upon dearomatization, in agreement with the increased double bond character of the C–C bond. Although the N–C bonds within the naphthyridine core do elongate upon dearomatization as expected, the trend is less clear. Together, our findings fit well with the resonance structures for each protonation state of the PNNP ligand depicted in Scheme 1.

Complex **3** is thermally stable but readily reacts with traces of proton sources to give **2**. In agreement with this observation, treatment of **3** with one equiv of Et_3NHCl results in quantitative formation of **2**. To explore whether the $t\text{-BuPNNP}^{**}$ ligand enables cooperative bond activation we placed a $[\text{D}_8]\text{THF}$ solution of **3** under an atmosphere of H_2 . Excitingly, we observed full conversion of **3** over the course of 30 h at 40°C concomitant with formation of hydride complex **4** (Scheme 5) in 79% spectroscopic yield. Complex **4** was also independently synthesized in 67% yield by reacting **2** with Ph_2SiH_2 , which is converted to $\text{Ph}_2\text{SiHO}t\text{-Bu}$ according to ^1H NMR spectroscopy and GC-MS analysis. The single crystal X-



Scheme 5. Cooperative H₂ activation by **3** to give complex **4**.

ray structure revealed a tetranuclear “butterfly-shaped” copper cluster featuring two ^t-BuPNNP* ligands (Figure 2). The two Cu atoms within each ^t-BuPNNP* ligand are separated by 2.5106(6) and 2.5122(6) Å, which are similar to the distance between the Cu atoms in each non-dearomatized PN pocket [Cu21...Cu22 2.4778(5) Å]. In contrast, the distance between the Cu atoms in the dearomatized PN pockets is approximately 0.9 Å longer [Cu11...Cu12 3.4144(6) Å], which results in the overall butterfly shaped tetracopper(I) core. Two hydrides that display a μ₃-binding mode on each side of the cluster were located in the difference-Fourier maps (Figure 2, bottom). The Cu–H distances were slightly shorter for the Cu atoms that are situated in the dearomatized pocket of the ^t-BuPNNP* ligands [Cu12...H2 1.61(4) Å and Cu11–H2 1.67(4) Å] than for the other Cu sites

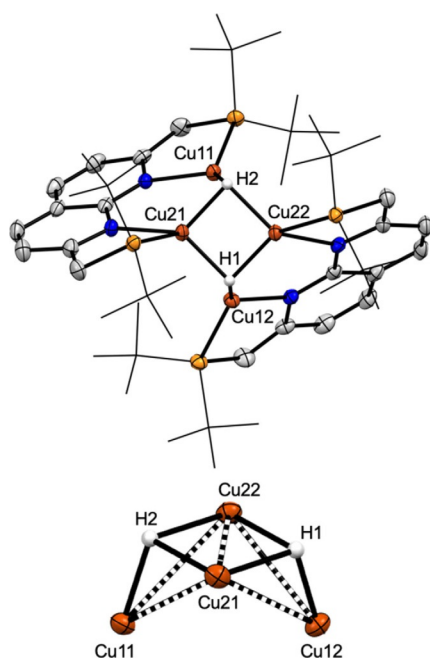


Figure 2. Displacement ellipsoid plots (50% probability) of **4** (top) and a depiction of the tetranuclear butterfly-shaped Cu core (bottom). Most hydrogen atoms are omitted and *t*-Bu groups on P are depicted as wireframe for clarity. Selected distances [Å] and angles [°]: Cu11...Cu21 2.5106(6), Cu11...Cu22 2.7310(6), Cu21...Cu22 2.4778(5), Cu21...Cu12 2.7338(6), Cu22...Cu12 2.5122(6), Cu11...Cu12 3.4144(6), Cu11–Cu21–Cu12 81.123(17), Cu11–Cu22–Cu12 81.149(17), Cu11–Cu21–Cu22 66.384(16), Cu12–Cu21–Cu22 57.385(15). Atoms Cu21, Cu22, H1, and H2 are approximately in one plane.

[1.76(4)–1.81(4) Å] in **4**. Although the experimental distances were not significantly ($>3\sigma$) different, the shorter Cu–H distances in the dearomatized PN pocket as well as the location of the hydrides were substantiated by DFT optimized geometries of **4**.^[14] Copper hydrides with fewer than six metal centers are uncommon^[21] and a CCSD search^[22] did not reveal any Cu₄H₂ butterfly-shaped clusters as featured in **4**. Given the prevalence of copper hydrides in catalysis,^[23] this unique tetranuclear dihydride architecture might enable distinct reactivity from other multinuclear hydrides, and we are currently exploring this.

The ¹H, ¹³C and ³¹P{¹H} NMR spectra of **4** in [D₈]THF or C₆D₆ at 298 K show the characteristic features of a partially dearomatized ^t-BuPNNP* ligand. Notably, in both solvents the ¹H NMR spectra show distinct resonances for each of the three protons on the methylene and methine linkers and four resonances for the *t*-Bu groups are observed, indicating that the CH₂ protons and *t*-Bu groups are diastereotopic. This shows that the mirror plane containing the expanded pincer plane is lost, implying that the tetranuclear complex assembly stays intact in solution. Although no hydride resonances were observed in the ¹H NMR spectra, the ²H NMR spectrum of a sample of **4** that was synthesized by reacting **2** with Ph₂SiD₂ showed a resonance at δ = 1.2 ppm (Figure S23, Supporting Information). This shows that the hydride resonance in the ¹H NMR spectrum is likely obscured by the resonances of the protons on the *t*-Bu groups.^[24] This same resonance was observed in the ²H NMR spectrum of a [D₈]THF solution of **3** that was exposed to an atmosphere of D₂ at 40 °C for 48 h (Figure S26, Supporting Information). Moreover, in the ¹H NMR spectrum both H–D and an equal decrease in the intensity of the CH and CH₂ resonances in the ligand arms was observed. This suggests a reversible cooperative activation of D₂ that results in partial D incorporation into the ligand arms, which was confirmed by ²H NMR analysis (Figure S27, Supporting Information). Notably, no H/D scrambling was observed upon heating a [D₈]THF solution of **4** (with or without KO*t*-Bu) under an atmosphere of D₂ at 40 °C, suggesting that the reversible cooperative bond activation step takes place prior to formation of the dimer **4**.

In conclusion, we prepared a new proton-responsive expanded pincer ligand, ^t-BuPNNP. The ligand can host two copper(I) centers and shuttle reversibly between three protonation states concomitant with partial or full dearomatization of the naphthyridine core. Moreover, the ^t-BuPNNP ligand enables cooperative H₂ activation on dicopper(I) and induces formation of a unique tetranuclear copper dihydride cluster. To the best of our knowledge, this work demonstrates the first example of metal–ligand cooperativity in naphthyridine-based bimetallic complexes, and of cooperative H₂ activation on copper. These studies further the development of new bimetallic systems that employ both metal–metal and metal–ligand cooperativity to activate chemical bonds. In addition to investigating the further reactivity of the systems reported herein, we are exploring various other avenues to discover if the ^t-BuPNNP ligand can be as valuable in bimetallic bond activation and catalysis as the lutidine-derived PNP analogues are in mononuclear chemistry.

Supporting information

CCDC 1919274, 1919275, 1919276, and 1919277 contain the supplementary crystallographic data for this paper. These data are provided free of charge by The Cambridge Crystallographic Data Centre.

NMR data files can be found under <https://doi.org/10.4121/uuid:9ee9204c-2da8-480d-a06e-f6433aaeaa83>.

Acknowledgements

This work was supported by The Netherlands Organization for Scientific Research (START-UP grant 740.018.019 to D.L.J.B.) and the European Union Horizon 2020 research and innovation program (agreement 840836, D.L.J.B. MSCA-IF to, BiMetaCat). Access to supercomputer facilities was sponsored by NWO Exacte en Natuurwetenschappen (Physical Sciences). The X-ray diffractometer was financed by the NWO. Gerard van Koten, Bert Klein-Gebbink and Marc-Etienne Moret are acknowledged for valuable discussions and suggestions.

Conflict of interest

The authors declare no conflict of interest.

Keywords: bimetallics · copper hydride · ligand design · metal–ligand cooperativity · metal–metal interactions

- [1] a) D. Sippel, M. Rohde, J. Netzer, C. Trncik, J. Gies, K. Grunau, I. Djurdjevic, L. Decamps, S. L. A. Andrade, O. Einsle, *Science* **2018**, *359*, 1484–1489; b) M. Can, F. A. Armstrong, S. W. Ragsdale, *Chem. Rev.* **2014**, *114*, 4149–4174; c) W. Lubitz, H. Ogata, O. Rüdiger, E. Reijerse, *Chem. Rev.* **2014**, *114*, 4081–4148; d) M. D. Wodrich, X. Hu, *Nat. Rev. Chem.* **2017**, *2*, 0099.
- [2] a) L. Alig, M. Fritz, S. Schneider, *Chem. Rev.* **2019**, *119*, 2681–2751; b) J. R. Khusnutdinova, D. Milstein, *Angew. Chem. Int. Ed.* **2015**, *54*, 12236–12273; *Angew. Chem.* **2015**, *127*, 12406–12445; c) J. I. van der Vlugt, *Eur. J. Inorg. Chem.* **2012**, 363–375; d) D. L. DuBois, *Inorg. Chem.* **2014**, *53*, 3935–3960.
- [3] a) *Organometallic Pincer Chemistry*, Vol. 40 (Eds.: G. van Koten, D. Milstein), Springer, Berlin, **2013**; b) *The Chemistry of Pincer Compounds* (Eds.: D. Morales-Morales, C. Jensen), Elsevier Science, Amsterdam, **2007**.
- [4] For reviews see: a) D. Milstein, *Philos. Trans. R. Soc. London Ser. A* **2015**, *373*, 20140189; b) C. Gunanathan, D. Milstein, *Acc. Chem. Res.* **2011**, *44*, 588–602; c) J. I. van der Vlugt, J. N. H. Reek, *Angew. Chem. Int. Ed.* **2009**, *48*, 8832–8846; *Angew. Chem.* **2009**, *121*, 8990–9004.
- [5] a) R. B. Ferreira, L. J. Murray, *Acc. Chem. Res.* **2019**, *52*, 447–455; b) I. G. Powers, C. Uyeda, *ACS Catal.* **2017**, *7*, 936–958; c) N. P. Mankad, *Chem. Eur. J.* **2016**, *22*, 5822–5829; d) M. Iglesias, E. Sola, L. A. Oro in *Homo- and Heterobimetallic Complexes in Catalysis: Cooperative Catalysis* (Ed.: P. Kalck), Springer International Publishing, Cham, **2016**; pp. 31–58; e) K. M. Gramigna, D. A. Dickie, B. M. Foxmand, C. M. Thomas, *ACS Catal.* **2019**, *9*, 3153–3164; f) T. Ouyang, H.-J. Wang, H.-H. Huang, J.-W. Wang, S. Guo, W.-J. Liu, D.-C. Zhong, T.-B. Lu, *Angew. Chem. Int. Ed.* **2018**, *57*, 16480–16485; *Angew. Chem.* **2018**, *130*, 16718–16723; g) E. K. van den Beuken, B. L. Feringa, *Tetrahedron* **1998**, *54*, 12985–13011.
- [6] a) C. He, A. M. Barrios, D. Lee, J. Kuzelka, R. M. Daavdyov, S. J. Lippard, *J. Am. Chem. Soc.* **2000**, *122*, 12683–12690; b) C. He, J. L. Dubois, B. Hedman, K. O. Hodgson, S. J. Lippard, *Angew. Chem. Int. Ed.* **2001**, *40*, 1484–1487; *Angew. Chem.* **2001**, *113*, 1532–1535; c) J. K. Bera, N. Sadhukhanb, M. Majumdar, *Eur. J. Inorg. Chem.* **2009**, 4023–4038; d) M. S. Ziegler, K. V. Lakshmi, T. D. Tilley, *J. Am. Chem. Soc.* **2017**, *139*, 5378–5386.
- [7] M. S. Ziegler, D. S. Levine, K. V. Lakshmi, T. D. Tilley, *J. Am. Chem. Soc.* **2016**, *138*, 6484–6491.
- [8] M. S. Ziegler, N. A. Torquato, Levine, D. S. A. Nicolay, H. Celik, T. D. Tilley, *Organometallics* **2018**, *37*, 2807–2823.
- [9] T. C. Davenport, T. D. Tilley, *Angew. Chem. Int. Ed.* **2011**, *50*, 12205–12208; *Angew. Chem.* **2011**, *123*, 12413–12416.
- [10] Selected examples: a) I. G. Powers, J. M. Andjaba, X. Luo, J. Mei, C. Uyeda, *J. Am. Chem. Soc.* **2018**, *140*, 4110–4118; b) D. R. Hartline, M. Zeller, C. Uyeda, *J. Am. Chem. Soc.* **2017**, *139*, 13672–13675; c) S. Pal, Y.-Y. Zhou, C. Uyeda, *J. Am. Chem. Soc.* **2017**, *139*, 11686–11689; d) S. Pal, C. Uyeda, *J. Am. Chem. Soc.* **2015**, *137*, 8042–8045.
- [11] Y.-Y. Zhou, C. Uyeda, *Science* **2019**, *363*, 857–862.
- [12] Reviews on redox-active ligands: a) V. K. K. Praneeth, M. R. Ringenberg, T. R. Ward, *Angew. Chem. Int. Ed.* **2012**, *51*, 10228–10234; *Angew. Chem.* **2012**, *124*, 10374–10380; O. R. Luca, R. H. Crabtree, *Chem. Soc. Rev.* **2013**, *42*, 1440–1459; D. L. J. Broere, R. Plessius, J. I. van der Vlugt, *Chem. Soc. Rev.* **2015**, *44*, 6886–6915.
- [13] Based on the work described here, we anticipate that a recently reported ligand by the Tilley group could also display chemical noninnocence: A. Nicolay, T. D. Tilley, *Chem. Eur. J.* **2018**, *24*, 10329–10333.
- [14] See the Supporting Information for additional details.
- [15] T. Simler, L. Karmazin, C. Bailly, P. Braunstein, A. A. Danopoulos, *Organometallics* **2016**, *35*, 903–912.
- [16] a) S. Y. de Boer, Y. Gloaguen, M. Lutz, J. I. van der Vlugt, *Inorg. Chim. Acta* **2012**, *380*, 336–342; b) J. I. van der Vlugt, E. A. Pidko, R. C. Bauer, Y. Gloaguen, M. K. Rong, M. Lutz, *Chem. Eur. J.* **2011**, *17*, 3850–3854.
- [17] A. Marker, M. J. Gunter, *J. Magn. Reson.* **1982**, *47*, 118–132.
- [18] Reactions with 1 equiv KOt-Bu yielded an inseparable mixture of **1**, **2** and presumably PNNP*Cu₂Cl.
- [19] a) A. Nerush, M. Vogt, U. Gellrich, G. Leitus, Y. Ben-David, D. Milstein, *J. Am. Chem. Soc.* **2016**, *138*, 6985–6997; b) M. Vogt, A. Nerush, M. A. Iron, G. Leitus, Y. Diskin-Posner, L. J. W. Shimon, Y. Ben-David, D. Milstein, *J. Am. Chem. Soc.* **2013**, *135*, 17004–17018; c) J. I. van der Vlugt, E. A. Pidko, D. Vogt, M. Lutz, A. L. Spek, *Inorg. Chem.* **2009**, *48*, 7513–7515; d) J. I. van der Vlugt, M. Lutz, E. A. Pidko, D. Vogt, A. L. Spek, *Dalton Trans.* **2009**, 1016–1023.
- [20] There are only two examples of structurally characterized complexes featuring a doubly deprotonated PNP pincer ligand: M. Vogt, O. Rivada-Wheelaghan, M. A. Iron, G. Leitus, Y. Diskin-Posner, L. J. W. Shimon, Y. Ben-David, D. Milstein, *Organometallics* **2013**, *32*, 300–308; T. Simler, G. Frison, P. Braunstein, A. A. Danopoulos, *Dalton Trans.* **2016**, *45*, 2800–2804.
- [21] a) S. Zhang, H. Fallah, E. J. Gardner, S. Kundu, J. A. Bertke, T. R. Cundari, T. H. Warren, *Angew. Chem. Int. Ed.* **2016**, *55*, 9927–9931; *Angew. Chem.* **2016**, *128*, 10081–10085; b) A. W. Cook, Nguyen, T. D. W. R. Buratto, G. Wu, T. W. Hayton, *Inorg. Chem.* **2016**, *55*, 12435–12440; c) C. M. Wyss, B. K. Tate, J. Bacsa, T. G. Gray, J. P. Sadighi, *Angew. Chem.* **2013**, *125*, 13158–13161; d) G. D. Frey, B. Donnadiou, M. Soleilhavoup, G. Bertrand, *Chem. Asian J.* **2011**, *6*, 402–405; e) Z. Mao, J.-S. Huang, C.-M. Che, N. Zhu, S. K.-Y. Leung, Z.-Y. Zhou, *J. Am. Chem. Soc.* **2005**, *127*, 4562–4563.
- [22] A single compound was found that features a Cu₂H₂ core in which all copper sites are in the same plane unlike the butterfly shaped geometry in **4**: T. Nakajima, Y. Kamiroy, K. Hachiken, K. Nakamae, Y. Ura, T. Tanase, *Inorg. Chem.* **2018**, *57*, 11005–11018.
- [23] C. Deutsch, N. Krause, B. H. Lipshutz, *Chem. Rev.* **2008**, *108*, 2916–2927.
- [24] The chemical shifts of the μ₃-hydride in **4** falls within the range from 3.10 to –1.28 ppm observed for structurally characterized copper clusters containing μ₃-H ligands: a) J. Li, J. M. White, R. J. Mulder, G. E. Reid, P. S. Donnelly, R. A. J. O'Hair, *Inorg. Chem.* **2016**, *55*, 9858–9868; b) K. Nakamae, M. Tanaka, B. Kure, T. Nakajima, Y. Ura, T. A. Tanase, *Chem. Eur. J.* **2017**, *23*, 9457–9461, and Ref. [22].

Manuscript received: August 14, 2019

Accepted manuscript online: August 19, 2019

Version of record online: September 24, 2019